

## NEW HEURISTIC DIFFRACTION COEFFICIENT FOR MODELING OF WIRELESS CHANNEL

S. Soni and A. Bhattacharya

Department of Electronics and Electrical Communication Engineering  
IIT Kharagpur  
India

**Abstract**—A new reciprocal heuristic diffraction coefficient for lossy dielectric wedge is presented which is applicable to arbitrary positions of transmitter and receiver in a complex channel environment. The prediction obtained using proposed coefficient is compared with those obtained using rigorous Maliuzhinets' solution. The comparison shows significant improvement over available heuristic coefficients. The coefficient is valid for both parallel and perpendicular polarizations. Further, the measurement of the electric field in the vicinity of edge of the building is carried out, and the measurement result, thus obtained, is compared with predictions using the proposed coefficient.

### 1. INTRODUCTION

Success of mobile radio communication highly depends on accurate prediction of intermediate channel. In this context, deterministic propagation modeling is becoming a potential tool to accurately model dense urban scenario [1]. Deterministic model involves: (i) approximation of the individual urban scatterers by geometries for which canonical solutions are available, (ii) application of ray tracing tool. Geometrical Theory of Diffraction (GTD) [2] and its extension Uniform Theory of Diffraction (UTD) [3] are two extensively used tools to deterministically model diffraction phenomenon in propagation channel. Heuristic extension of UTD for dielectric wedge was proposed by Luebbers [4] to incorporate wedge with different conductivity and permittivity. Holm [5] further improved the coefficient by redefining the multiplying factor of the coefficient and also included additional term to consider the case of grazing incidence. This resulted in the coefficient that was close to the accurate rigorous Maliuzhinets

---

Corresponding author: S. Soni (sanjoo.ksoni@yahoo.co.uk).

coefficient [6] in the deep shadow region. However, in the illumination region, it was not accurate. In addition to that, it did not satisfy reciprocity requirement. El-Sallabi et al. [7] modified the coefficient by defining the incident and reflected angle used in the calculation of Fresnel reflection coefficient. The coefficient was close to the rigorous solution, however, it was not reciprocal. Daniela et al. [8] modified the Holm's coefficient by considering the reflection angle as suggested by Aidi et al. [9]. The coefficient was reciprocal only when the transmitter (Tx) and receiver (Rx) were on opposite side of the wedge. The coefficient was in good agreement with the Maliuzhinets' solution, however, it still lacks accuracy in some particular regions e.g., in deep shadow region [8, Fig. 5] and illumination region [8, Fig. 2, Fig. 3]. Moreover, the coefficient was compared with Maliuzhinets' solution for right-angle wedge case only.

For the case of impenetrable wedges with impedance boundary conditions, rigorous solutions are introduced by Maliuzhinets [6] and presented in UTD-like form in [12, 13] for the incidence of a plane wave and line source illumination respectively. However, these solutions led to rather involved formulations are applicable only to limited number of canonical configurations. For a wedge with arbitrary angle, the Maliuzhinets special function is cumbersome to compute which is a major deterrent to the use of rigorous theory of diffraction [6, 12, 13] in propagation prediction tools for wireless communication.

In this paper, we define reflection angles to calculate Fresnel reflection coefficient used in the computation of the diffraction coefficient and their regions of applicability in the entire exterior angle range of wedge such that overall the coefficient becomes efficient and perfectly reciprocal.

This paper is organized as follows: Section 2 discusses briefly about diffraction coefficients of Holm [5], Daniela [8]. Section 3 deals with novel proposed diffraction coefficient. In section 4, detailed numerical discussion is given and proposed solution is compared with our measurement and published measurement. Section 5 concludes the work.

## 2. HEURISTIC DIFFRACTION COEFFICIENT

### 2.1. Holm's Heuristic Diffraction Coefficient

In [5], Holm proposed a modification to the Luebbers' coefficient which resulted in good agreement in the deep shadow region. Holm's soft (s) and hard (h) heuristic coefficient are given as:

$$D^{s,h} = G_n^{s,h} [M_1 D_1 + M_4 D_4] + G_0^{s,h} [M_2 D_2 + M_3 D_3] \quad (1)$$

The components  $D_i (i = 1, \dots, 4)$  of diffraction coefficient in [3] are defined as:

$$D_{1,2} = -\frac{e^{-j\pi/4}}{2n\sqrt{2\pi k} \sin(\beta_0)} \cot\left(\frac{\pi \pm (\phi - \phi')}{2n}\right) F[kla^\pm(\phi - \phi')]$$

$$D_{3,4} = -\frac{e^{-j\pi/4}}{2n\sqrt{2\pi k} \sin(\beta_0)} \cot\left(\frac{\pi \pm (\phi + \phi')}{2n}\right) F[kla^\pm(\phi + \phi')] \quad (2)$$

where

$$M_1 = R_0^{s,h}(\theta_0)R_n^{s,h}(\theta_n), \quad M_2 = 1,$$

$$M_3 = R_n^{s,h}(\theta_n) \quad \text{and} \quad M_4 = R_0^{s,h}(\theta_n)$$

$R_0^{s,h}$  and  $R_n^{s,h}$  are the Fresnel reflection coefficient for 0-face and  $n$ -face of dielectric wedge and are given as:

$$R_{o,n}^s = \frac{\sin(\theta_{o,n}) - \sqrt{\varepsilon - \cos^2 \theta_{o,n}}}{\sin(\theta_{o,n}) + \sqrt{\varepsilon - \cos^2 \theta_{o,n}}}, \quad R_{o,n}^h = \frac{\varepsilon \sin(\theta_{o,n}) - \sqrt{\varepsilon - \cos^2 \theta_{o,n}}}{\varepsilon \sin(\theta_{o,n}) + \sqrt{\varepsilon - \cos^2 \theta_{o,n}}}$$

$$\varepsilon = \varepsilon_r - j\frac{\sigma}{(2\pi f \varepsilon_0)}$$

$\sigma$  = Conductivity (S/m),  $f$  = Frequency (Hz),  $\varepsilon_r$  = Relative permittivity.

Incidence angle  $\theta_0$  and  $\theta_n$  are defined as:

$$\theta_0 = \min(\phi', \phi), \quad \theta_n = \min(n\pi - \phi', n\pi - \phi) \quad (3)$$

Here, the angles  $\phi'$  and  $\phi$  are the incident and diffracted angle as defined in Fig. 1. The factor  $G_0^{s,h}$  and  $G_n^{s,h}$ , to account for grazing incidence, are as follows:

$$G_0^{s,h} = G_n^{s,h} = 1/2, \quad \phi' = 0 \text{ or } \phi' = n\pi$$

$$G_0^{s,h} = G_n^{s,h} = 1, \quad \text{otherwise} \quad (4)$$

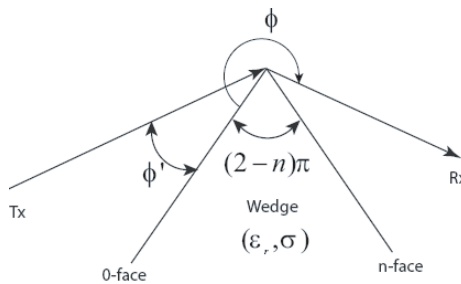


**Figure 1.** Geometry for diffraction by a dielectric wedge.

## 2.2. Daniela Heuristic Diffraction Coefficient

In [8], Daniela modified the Holms coefficient in order to make it reciprocal. Moreover, the definition of incident and reflected angle was taken as suggested by Aidi et al.. The definition of angles proposed by Aidi et al. is [9]

$$\theta_0 = \theta_n = \min(\phi', \phi, n\pi - \phi', n\pi - \phi)$$

With this definition of angles, the diffraction coefficient proposed by Daniela et al. [8] is given as:

$$D^{s,h} = G_n^{s,h} [M_1 D_1 + M_3 D_3] + G_0^{s,h} [M_2 D_2 + M_4 D_4] \quad (5)$$

where  $D_i (i = 1, \dots, 4)$  are defined in (2) and  $G_0^{s,h}$  and  $G_n^{s,h}$  are related with the grazing incidence and are defined in (4). Reciprocity imposes  $M_1, M_2$  to be arranged as:

$$M_1 = \begin{cases} R_0^{s,h} R_n^{s,h} & \phi' < n\pi/2 \\ 1, & \phi' \geq n\pi/2 \end{cases}$$

$$M_2 = \begin{cases} 1, & \phi' < n\pi/2 \\ R_0^{s,h} R_n^{s,h}, & \phi' \geq n\pi/2 \end{cases}$$

and  $M_3 = R_n^{s,h}, M_4 = R_0^{s,h}$ .

Using the arrangement as described above, and by adopting the definition of incidence angle, better accuracy was achieved and coefficient was reciprocal when the Transmitter (Tx) and Receiver (Rx) are on either side of wedge faces. However, it was not reciprocal when both the Tx and Rx were on the same side of faces.

## 3. NOVEL HEURISTIC DIFFRACTION COEFFICIENT

In this approach, we are dividing the complete exterior angle  $n\pi$  in three parts. The region-1 is  $(\phi + \phi') \leq \pi$  and region-2 is  $(\phi + \phi') < \pi \cap \phi \leq (2n - 1)\pi - \phi'$  and region-3 is  $\phi > (2n - 1)\pi - \phi'$ . The division of these three region is based on the position of reflection shadow boundaries (RSB) for 0-face and  $n$ -face of the wedge [3] and definition of angles is based on the requirement of accuracy of heuristic coefficient in the corresponding region and also noting that it makes the coefficient perfectly reciprocal. The following table summarizes these regions and definition of incidence and reflected angle in each of the region:

**Table 1.** Definition of angle involved in the calculation of Fresnel Reflection coefficient.

Region-1: $(\phi + \phi') < \pi$	$\theta_0 = \frac{\pi}{2} - \left  \frac{\pi}{2} - \phi' \right $ $\theta_n = \frac{\pi}{2} - \left  \frac{\pi}{2} - \phi \right $
Region-2: $(\phi + \phi') > \pi \cap$ $\phi \leq (2n - 1)\pi - \phi'$	$\theta_0 = \min(\phi', \phi, n\pi - \phi', n\pi - \phi)$ $\theta_n = \theta_0$
Region-3: $\phi > (2n - 1)\pi - \phi'$	$\theta_0 = \frac{\pi}{2} - \left  \frac{\pi}{2} - (n\pi - \phi') \right $ $\theta_n = \frac{\pi}{2} - \left  \frac{\pi}{2} - (n\pi - \phi) \right $

To meet reciprocity, the multiplying factor is arranged as follows:  
For region-1 and region-3, reciprocity imposes following conditions:

$$\left. \begin{matrix} M_1 = R_0^{s,h} R_n^{s,h} \\ M_2 = 1 \\ M_3 = R_n^{s,h} \\ M_4 = R_0^{s,h} \end{matrix} \right\} \phi \geq \phi' \quad \left. \begin{matrix} M_1 = 1 \\ M_2 = R_0^{s,h} R_n^{s,h} \\ M_3 = R_0^{s,h} \\ M_4 = R_n^{s,h} \end{matrix} \right\} \phi < \phi' \quad (6)$$

and in the region-2, reciprocity requires:

$$\left. \begin{matrix} M_2 = 1, \\ M_1 = R_0^{s,h}(\theta_0) R_n^{s,h}(\theta_n), \\ M_3 = M_4 = R_0^{s,h}(\theta_0) = R_n^{s,h}(\theta_n) \end{matrix} \right\} (\phi - \phi') \geq 0 \quad (7)$$

$$\left. \begin{matrix} M_2 = R_0^{s,h}(\theta_0) R_n^{s,h}(\theta_n), \\ M_1 = 1, \\ M_3 = M_4 = R_0^{s,h}(\theta_0) = R_n^{s,h}(\theta_n) \end{matrix} \right\} (\phi - \phi') < 0$$

Here,  $R_0^{s,h}$  and  $R_n^{s,h}$  are calculated using the incidence and diffracted angle as defined in the above Table 1. Note that in the second region,  $R_0^{s,h}$  and  $R_n^{s,h}$  are calculated using incident angle  $\theta_0$  and  $\theta_n$  as per Aidi and Lavergnat angular definition [9]. The justification of using these multiplying factors is as follows:

Reciprocity requires that “Exchanging the position of the source and observation point must not change the diffraction coefficient (See Fig. 2) i.e.,

$$D(\phi, \phi') = D(\phi', \phi) \quad (8)$$

Following the definition of components of diffraction coefficient in (2), the condition in (8) results in:

$$\phi' \leftrightarrow \phi \Rightarrow \left\{ \begin{matrix} D_1 \leftrightarrow D_2 \\ D_3 \text{ and } D_4 \text{ remain unchanged} \end{matrix} \right. \quad (9)$$

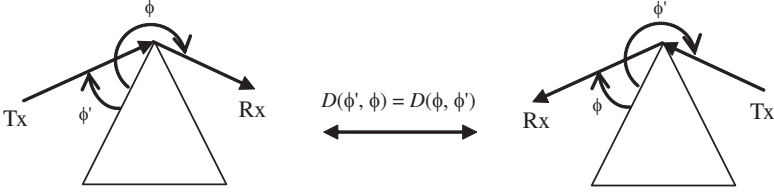


**Figure 2.** Reciprocity condition.

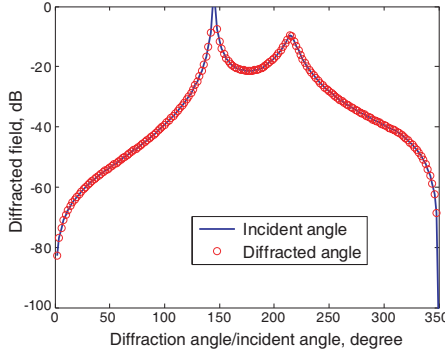


**Figure 3.** Reciprocal property of proposed coefficient.

Hence condition for reciprocity requires that:

$$\begin{aligned} M_{1,2}(\phi, \phi') &= M_{2,1}(\phi', \phi) \\ M_{3,4}(\phi, \phi') &= M_{3,4}(\phi', \phi) \end{aligned} \quad (10)$$

Considering the diffraction coefficient parameters  $D_i (i = 1, \dots, 4)$  in (2), we see that for region-1 and region-3,  $\phi' \leftrightarrow \phi$  leads to  $D_1 \leftrightarrow D_2$  while  $D_3, D_4$  remain unchanged. Further, the reflection coefficients  $R_0$  and  $R_n$  are also mutually interchanged (See Table 1). Hence, in order that overall diffraction coefficient remains unchanged, multiplying factors of  $D_1$  and  $D_2$  need to be interchanged. Similarly, multiplying factors of  $D_3$  and  $D_4$  should also be interchanged. For region-2, multiplying factors of  $D_3$  and  $D_4$  will remain same in either of the cases and hence need not be interchanged and multiplying factors of only  $D_1$  and  $D_2$  need to be interchanged.

The above arrangement makes the coefficient perfectly reciprocal as shown in the Fig. 3. Here, in the first case, wedge angle is taken to be  $10^\circ$  and for given incident angle of  $35^\circ$ , observation point is moved in a circle of radius 1.5 m with tip of wedge as a centre. In the second case, the source and observation points were interchanged and keeping observation point constant at  $35^\circ$ , source is moved in a circle with

same radius as in previous case. From the Fig. 3, it is quite obvious that diffracted field in both of the cases is exactly same, thus, making coefficient perfectly reciprocal.

## 4. NUMERICAL RESULT

### 4.1. Comparison with Accurate Rigorous Maliuzhinets Diffraction Coefficient

In this section, usefulness of novel coefficient is demonstrated. The novel coefficient is compared with accurate rigorous Maliuzhinets' solution as a reference. Maliuzhinets' solution is obtained using [12, (9)] where rigorous solution is presented in UTD-like form. Maliuzhinets special function used in [12, (9)] is obtained using numerical computation method described in [14, (7)]. The proposed coefficient is further compared with Holm's and Daniela coefficient in order to show improvement over latter two. The wedge is characterized with conductivity  $\sigma = 0.001 \text{ S/m}$  and  $\epsilon_r = 8$ . Operating frequency is 5 GHz. The distance of source and observation point was taken to be 1.5 m each from the tip of wedge. Keeping the source at given angle, the observation point was moved at the step of  $3^\circ$  to obtain diffracted field. In order to show reciprocity, the source point and observation point were interchanged and keeping observation point at given angle, source point was moved at the step of  $3^\circ$ . Edge tip was the centre of the circle. For comparison purpose, the wedge angle is chosen to be  $90^\circ$  and  $150^\circ$ . Both the TM (Soft) and TE (Hard) polarization are considered.

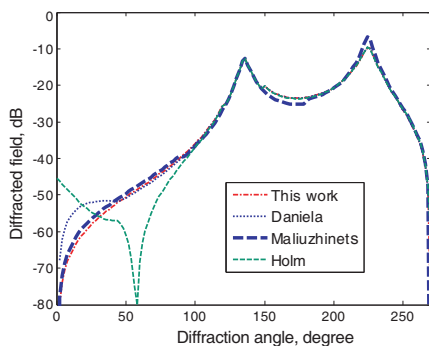


**Figure 4.** Comparison of different diffraction coefficients (wedge angle is  $90^\circ$  and  $\phi' = 45^\circ$ , TM polarization).

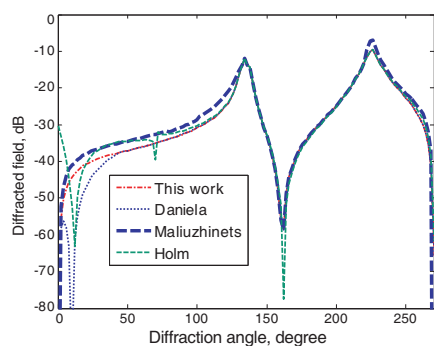


**Figure 5.** Comparison of different diffraction coefficients (wedge angle is  $90^\circ$  and  $\phi' = 45^\circ$ , TE polarization).

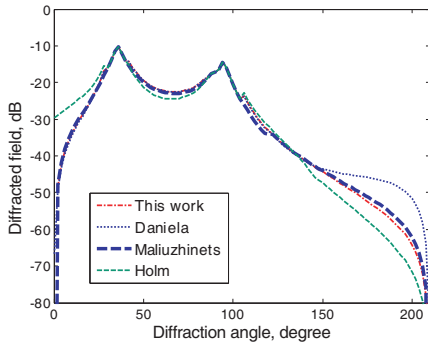


**Figure 6.** Comparison of different diffraction coefficients (wedge angle is  $150^\circ$  and  $\phi' = 145^\circ$ , TM polarization).

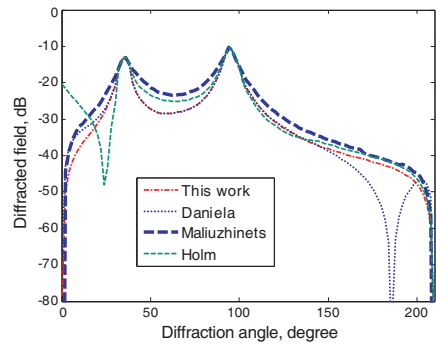


**Figure 7.** Comparison of different diffraction coefficients (wedge angle is  $150^\circ$  and  $\phi' = 145^\circ$ , TE polarization).

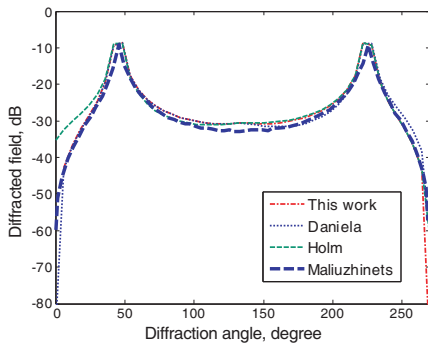


**Figure 8.** Comparison of different diffraction coefficients (wedge angle is  $90^\circ$  and  $\phi' = 135^\circ$ , TM polarization).

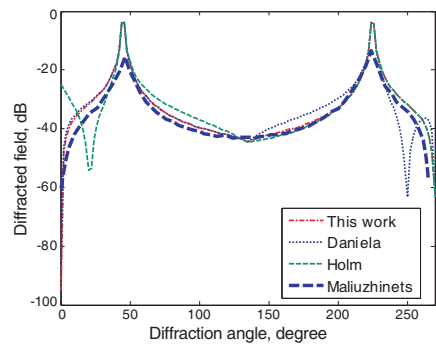


**Figure 9.** Comparison of different diffraction coefficients (wedge angle is  $90^\circ$  and  $\phi' = 135^\circ$ , TE polarization).

In the present analysis, the wedges are taken to be  $90^\circ$  and  $150^\circ$  and incident angles are  $45^\circ$ ,  $135^\circ$  and  $145^\circ$ . Diffracted field is calculated using the formula  $E_d = D^* \exp(-jkr_2)/\sqrt{r_2}$  with  $r_2$  a distance from wedge tip to observation point and unit incident field is considered at wedge diffraction point. Fig. 4 and Fig. 5 show the diffracted field pattern for the  $90^\circ$  wedge and incident angle  $45^\circ$  with both TM and TE polarization. Here, a clear improvement can be seen in illumination region where both Holm and Daniela are differing from Maliuzhinets coefficient. Figs. 6 and 7 are for the  $150^\circ$  wedge and incidence angle  $145^\circ$ . In this scenario, the novel coefficient gives better result in

deep shadow region where Daniela result is differing significantly in deep shadow region. In other region, predictions of all coefficients are almost same except Holm which gives poor prediction in illumination region. Figs. 8 and 9 show the comparison of proposed coefficient with other heuristic coefficients for  $90^\circ$  wedge angle and incident angle  $135^\circ$ . A clear improvement can be seen in deep shadow region especially in Fig. 9 where Daniela coefficient shows sharp discrepancy with Maliuzhinets' solution.

#### 4.2. Comparison with Measurement

The measurement was carried out to verify the accuracy of the proposed diffraction coefficient. To reduce the influence of unwanted factor, the building site was chosen to be isolated building where nearby there was no scattering objects such as tree, pole etc.

The experiments consisted of measurement of path loss due to presence of building between Tx and Rx antennas. The rooftop diffraction was neglected as the transmitter and receiver heights were much smaller than building height. The area immediately adjacent to the building was also flat. This made measurement track layout easy. The layout of measurement planning is given in Fig. 10 and Fig. 11 shows the photograph of building site where measurement was carried out.

Measurement was taken at every 1m along the track starting from line-of-sight (LOS) where direct, reflected and diffracted rays were present, crossing the shadow boundary and entering well in the shadow region where only diffracted fields were present.

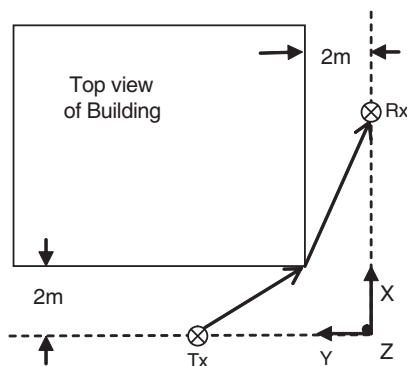


**Figure 10.** Layout of measurement site (2D view): Height of transmitter  $h_t = 2\text{ m}$ , height of receiver  $h_r = 1.8\text{ m}$ .



Figure 11. Photograph of measurement site.

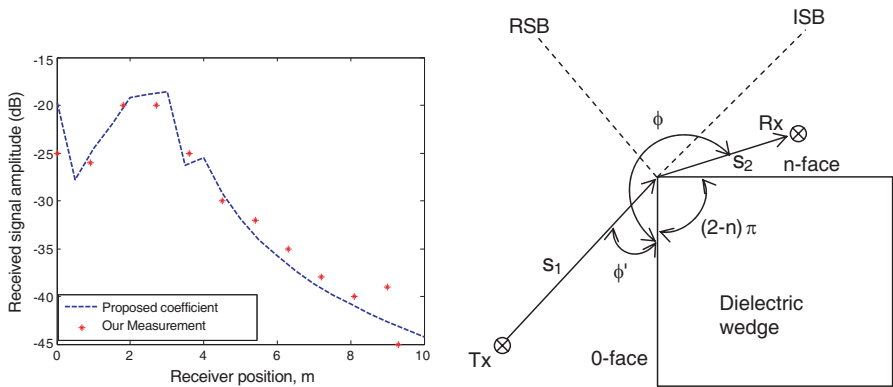


Figure 12. Comparison of prediction of received field amplitude with measurement (vertical polarization).

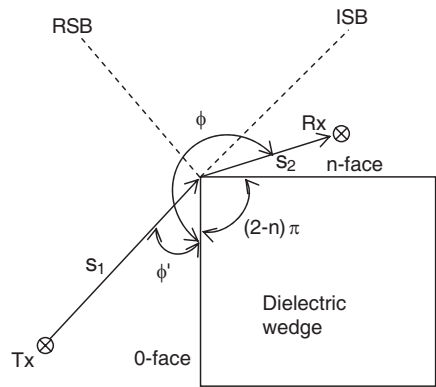


Figure 13. Diffraction by wedge with wedge angle  $90^\circ$  [10, Fig. 10].

The measurement set up used in this paper includes a wideband signal generator (9 kHz–3.3 GHz) that operates at 900 MHz with signal output 10 dBm and is capable of producing CW, AM, FH and pulse modulated signal. An amplifier (10 MHz–26.5 GHz) with 20 dB gain was used to boost up signal level from +10 dBm to 30 dBm and high precision Spectrum analyzer (N1996A, 100 kHz–3 GHz) was used to record the field strength of received signal.

In order to ensure that no unwanted signal is interfering with our frequency of operation, the data were recorded when RF was ON and when RF was OFF. When RF was OFF, the signal level fell to noise margin indicating the absence of any other signal at our frequency of operation.

Figure 12 shows the predicted and the measured result of the electric field strength in the shadow of building. For the prediction, the proposed diffraction coefficient was used with ray tracing. The wall material was modeled with conductivity  $\sigma = 1 \times 10^{-3} \text{ S/m}$  and relative permittivity  $\epsilon_r = 6$ . The value of  $\epsilon_r$  is consistent with the range  $5 \leq \epsilon_r \leq 7$  suggested by measurement in [11]. Rooftop diffracted signal is ignored as the transmitter and receiver heights are much smaller than the building heights. It is noted that there is good agreement between prediction results and the measured data.

### 4.3. Comparison with Published Measurement [10]

To further validate the proposed coefficient, the comparison is made with published measurement in [10]. Here, the diffraction from right-angled brick wedge with conductivity  $\sigma = 0.01 \text{ S/m}$  and relative permittivity of  $\epsilon_r = 4.0$  is considered. Transmitter is a vertically polarized, ground based open ended wave guide fed with 30 GHz CW constant level signal. Incident angle of source is  $\phi' = 5^\circ$  and the edge is 1.5m away from transmitter. The observation point is moved along a circular path and measurements are taken at a distance of  $s_2 = 10\lambda = 0.01 \text{ m}$  as shown in Fig. 13. Fig. 14 shows comparison between predicted field strength obtained by proposed coefficient and published measurement in [10]. We see that the prediction is in good agreement with measurements.

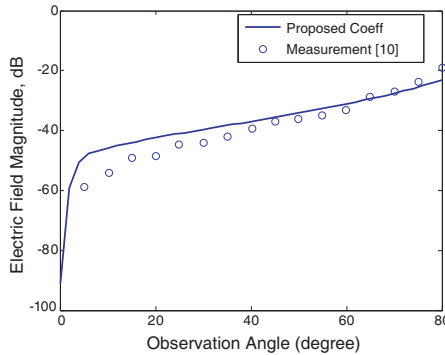


**Figure 14.** Comparison of prediction of electric field amplitude with published measurement [10], (vertical polarization).

## 5. CONCLUSION

In this paper, a novel heuristic diffraction coefficient is presented which is efficient and reciprocal. The coefficient is shown to agree well with the accurate rigorous Maliuzhinets' solution. Comparison has been made for right angle and non-right angle wedges. It is shown that the proposed coefficient is perfectly reciprocal and is more accurate than that of Daniela and Holm in both the illuminated and deep shadow regions. To further validate the coefficient, the measurement was carried out in the vicinity of building, and prediction is found to be in good agreement with the measurement. Finally, the predicted field strength is compared with the published measurement, and prediction is found to agree well with the measurement.

Thus, it is hoped that the proposed coefficient may find suitable application in modeling of radio propagation channel.

## ACKNOWLEDGMENT

The authors are thankful to Prof. S. Sanyal, Department of Electronics and Electrical Communication Engg. IIT Kharagpur, for valuable suggestion.

## REFERENCES

1. COST Action 273, "Mobile broadband multimedia networks techniques, models and tools for 4G," ISBN 0-12-369422-1, 2006.
2. Keller, J. B., "Geometrical theory of diffraction," *J. Opt. Soc. Amer.*, Vol. 52, No. 2, 116–130, Feb. 1962.
3. Kouyoumjian, R. G. and P. H. Pathak, "A uniform geometrical theory of diffraction for an edge in a perfectly conducting surface," *Proc. IEEE*, Vol. 62, No. 11, 1448–1461, Nov. 1974.
4. Luebbers, R. J., "Finite conductivity uniform GTD versus knife edge diffraction in prediction of propagation path loss," *IEEE Trans. Antennas Propagat.*, Vol. 32, No. 1, 70–76, Jan. 1984.
5. Holm, P., "A new heuristic UTD diffraction coefficient for non-perfectly conducting wedges," *IEEE Trans. Antennas Propagat.*, Vol. 48, No. 8, 1211–1219, Aug. 2000.
6. Maliuzhinets, G. D., "Excitation, reflection and emission of surface waves from a wedge with given face impedances," *Sov. Phys. Doklady*, Vol. 3, 752–755, 1958.
7. El-Sallabi, H. M. and P. Vainikainen, "Improvements to diffraction

- coefficient for non-perfectly conducting wedges,” *IEEE Trans. Antennas Propagat.*, Vol. 53, No. 9, 3105–3109, Sep. 2005.
8. Schettino, D. N., F. J. S. Moreira, K. L. Borges, and C. G. Rego, “Novel heuristic UTD coefficients for the characterization of radio channels,” *IEEE Transactions on Magnetics*, Vol 43, No. 4, 1301–1304, Apr. 2007.
  9. Aïdi, M. and J. Lavergnat, “Comparison of Luebbers’ and Maliuzhinets’ wedge diffraction coefficients in urban channel modelling,” *Progress In Electromagnetics Research*, PIER 33, 1–28, 2001.
  10. Remley, K. A., H. R. Anderson, and A. Weissnar, “Improving the accuracy of ray-tracing techniques for indoor propagation modeling,” *IEEE Trans. on Vehicular Technology*, Vol. 49, No. 6, 2350–2358, Nov. 2000.
  11. Landdron, O., M. J. Feuerstein, and T. S. Rappaport, “A comparison of theoretical and empirical reflection coefficients for typical exterior wall surfaces in mobile radio environment,” *IEEE Trans. Antennas Propagat.*, Vol. 44, No. 3, 341–351, Mar. 1996.
  12. Tiberio, R., G. Pelosi, and G. Manara, “A uniform GTD formulation for the diffraction by a wedge with impedance faces,” *IEEE Trans. Antennas Propagat.*, Vol. 33, No. 8, 867–873, Aug. 1985.
  13. Tiberio, R., G. Pelosi, and G. Manara and P. H. Pathak, “High-frequency scattering from a wedge with impedance faces illuminated by a line source — Part I: Diffraction,” *IEEE Trans. Antennas Propagat.*, Vol. 37, 212–218, Feb. 1989.
  14. Hu, J.-L., S.-M. Lin, and W.-B. Wang, “Calculation of Maliuzhinets function in complex region,” *IEEE Trans. Antennas Propagat.*, Vol. 44, No. 8, 1195–1196, Aug. 1996.